Polymer Vol. 38 No. 25, pp. 6097–6102, 1997

0032-3861/97/$17.00+0.00

PII: S0032-3861(97)00185-7

Colloidal and electrokinetic behaviour of poly(methyl methacrylate-*co*-butyl acrylate) latex particles

Elias Unzueta and Jacqueline Forcada
Grupo de Ingeniería Química, Departamento de Química Aplicada, Facultad de Ciencias Químicas, Universidad del País Vasco/Euskal Herriko Unibertsitatea, Apdo. 1072, 20080 San Sebastián/Donostia, Spain

and Roque Hidalgo-Álvarez*
Grupo de Física de Fluidos y Biocoloides, Departamento de Física Aplicada, Facultad de Ciencias, Universidad de Granada, 18071 Granada, Spain
(Received 30 June 1996; revised 23 January 1997)

Poly(methyl methacrylate-*co*-butyl acrylate) latex particles were synthesized by both seeded and unseeded semicontinuous emulsion copolymerization processes. Particle size and surface charge densities were characterized by TEM and potentiometric and conductimetric titrations, respectively. The electrophoretic mobilities of the latexes were studied at different ionic strength and constant pH and then at constant ionic strength and different pH. An investigation of the effect of surface density on ζ-potential is described. Conversion of mobility values into ζ potentials was accomplished according to the theory of Dukhin–Semenikhin in order to take anomalous surface conductance into account. The dimensionless relaxation factor (*Rel*) was calculated for the different surface charge density of the latexes obtained. The colloidal stability of the latex particles after addition of KBr at an appropriate concentration was followed monitoring the optical absorbance changes of the dispersion. The critical coagulation concentration (CCC) was obtained from the intersection points of the straight log W–log C line with the x-axis (stability factor vs. concentration). The stability factors of the synthesized latexes were measured at pH 5, 7 and 9. The results indicate that these latexes are electrostatically stabilized. © 1997 Elsevier Science Ltd.

(Keywords: emulsion copolymerization; latex particles; electrophoretic mobility)

INTRODUCTION

Polymer colloids play an important role in many industrial processes such as the production of synthetic rubber, surface coatings, adhesives, as additives in paper, in textiles and many other products. The polymerization process design has a direct effect on the properties of final latex.

The combination of rigid poly(methyl methacrylate), flexible poly(butyl acrylate) and readiness to copolymerize both in the desired composition allows the manufacturing of products with diverse and numerous applications. One of the most important is as a paint medium for coatings applied on many different substrates[1,2].

Semicontinuous emulsion copolymerization offers a great degree of operational flexibility. It permits high polymer quality (copolymer composition and particle size distribution) and reactor temperature control. The kinetics of the process can be adjusted by changing the operating conditions, above all, the reactant feeds.

Previous work[3] analysed the effects of the concentration and type of the surfactant systems on the kinetic features (conversion and copolymer composition) and colloidal characteristics (mean particle diameter and particle size distribution) in seeded semicontinuous emulsion copolymerization of methyl methacrylate and butyl acrylate. Moreover[4], in order to study the effect of the nature and concentration of the surfactant system on the nucleation process and on the growth and coagulation of polymer particles, unseeded semicontinuous emulsion copolymerization reactions were carried out.

For a proper understanding of the stability, rheology and many other properties of polymer colloid–liquid dispersions, a quantitative description of the charge and potential distribution around the particles is essential. The electrical aspects of the solid–liquid interfaces are particularly relevant because, under normal conditions used in practice, the electrical interactions can be substantial. Microelectrophoretic mobility is often a powerful tool for studying the electrokinetic characteristics of latex–aqueous solution interfaces[5–7].

The colloidal stability of the latexes was studied by measuring the stability factor vs. the concentration of KBr. This way one obtains the critical coagulation

* To whom correspondence should be addressed

concentration (CCC), which is an important constant at the time these polymer colloids are used in applications.

This work is a study of the electrokinetic behaviour and the colloidal stability of poly (methyl methacrylate-*co*-butyl acrylate) polymer particles synthesized by means of both seeded and unseeded emulsion copolymerization processes.

EXPERIMENTAL

Methyl methacrylate (MMA) and butyl acrylate (BuA) monomers were distilled under reduced nitrogen pressure. All the other materials were used as received. Potassium persulfate ($K_2S_2O_8$, Merck) and sodium dihydrogen phosphate monohydrate ($NaH_2PO_4H_2O$, Merck, Darmstadt, Germany) were used as initiator and buffer, respectively. The surfactants used were sodium lauryl sulfate (SLS, Merck), nonyl phenol polyethylene oxide phosphate (Gafac RE610, Gaf Chemicals, New Jersey, USA) and polyethylene oxide lauryl ether (Brij 35, ICI, Kortenberg, Belgium). Deionized water was used throughout.

Polymerizations were carried out in a 0.5 l glass reactor, fitted with a reflux condenser, stainless-steel stirrer, sampling device, nitrogen inlet and feed inlet tube.

Two kinds of semicontinuous emulsion copolymerizations were carried out, seeded and unseeded. Latexes were prepared at 60°C using the recipe given in *Table 1*. In seeded copolymerizations, the seeds were prepared at 80°C by means of a batch emulsion copolymerization of MMA and BuA. After polymerization, the seed was kept overnight at 90°C to decompose the initiator. The volume average diameters of the seeds used in the seeded polymerizations were 33 and 80 nm, calculated from their particle size distributions (PSDs).

The synthesis variables for the polymerization process were the initial charge added to the reactor at the beginning of the process and the nature of the surfactant system (anionic/nonionic) used (see *Table 2*). The feed was divided into two streams. One stream contained a mixture of both monomers in the required ratio, and the other a solution of initiator, surfactant (or surfactant system) and buffer in water.

To ensure monomer 'starved' conditions for the monomer in the reactor the flow rates of these streams were kept low and constant, homogeneous copolymer compositions (50/50 molar) were obtained during the reaction. The monomer and aqueous feed streams were calculated to last for 5.5 h after which, the polymerization was continued in batch for 1 h.

The obtained latexes were cleaned by serum replacement followed by ion exchange over a mixed bed. Surface charge densities were obtained by conductimetric and potentiometric titrations, the PSDs by transmission electron microscopy (TEM) on representative samples of more than 1000 particles. The average particle diameters were calculated from the PSD[3].

Table 3 shows calculated volume (d_v) and area (d_a) average diameters, polydispersity indexes (PDI) and surface charge densities (σ_o) for each of the synthesized latexes.

A Milton Roy Spectronic 601 spectrophotometer was used to determine the critical coagulation concentration (CCC). In a typical coagulation experiment, 2.4 ml of a buffered latex solution was put into the spectrophometer cell and the optical absorbance was measured. Potassium bromide (0.6 ml) of a given concentration was quickly added. The final particle concentration in the cell was 10^{10} part ml^{-1}. The optical absorbance (A) was measured immediately and its change vs. time (t) was recorded continuously for a period of 30 s. The curves were linear in the early stages of coagulation whatever the electrolyte concentration. The initial slope of such curve is directly proportional to the initial coagulation rate. Slopes increased with increasing electrolyte concentration until a maximum was reached: the critical coagulation concentration (CCC). At higher electrolyte concentrations there was no further increase. The slope at the CCC was taken as the fastest coagulation rate of the latex[8].

The stability factor (W) values for each electrolyte concentration (C_e) were calculated from $W = (dA/dt)_f/dA/dt)_s$ (where $(dA/dt)_f$ is the initial slope in fast coagulations and $(dA/dt)_s$ is the initial slope for lower electrolyte concentrations). Log W values were then plotted vs. log C_e. The CCC values from these curves are given in *Table 4*.

Electrophoretic mobilities were obtained with a Zeta–Sizer IIc (Malvern Instruments, Worcestershire, UK) by taking the average of three measurements at the stationary level in a cylindrical cell. Mobility measurements at different ionic strengths were made at constant pH equal to 6.0, and the measurements at different pH were made at constant ionic strength, 10^{-3} M.

All experiments were, at least, duplicated.

Table 1 Global recipe used in the copolymerization reactions

Reactant	Weight (g)
Water	225
MMA	65.78
BuA	84.22
Surfactant	4.5
$K_2S_2O_8$	0.15
$NaH_2PO_4H_2O$	0.15

Table 2 Initial charge and surfactant system used in each run

Run	Initial charge	Surfactant
E1	S (33 nm)	SLS + Gafac RE610
E3	S (33 nm) + M	SLS + Gafac RE610
E4	S (33 nm) + E	SLS + Gafac RE610
E9	S (33 nm) + E	SLS + Brij 35
EU	S (80 nm)	SLS + Gafac RE610
E2	E + W	SLS
EV	E + W + B + I	SLS + Gafac RE610
EAE	E + W + B + I	SLS + Gafac RE610

W = water, S = seed, E = surfactant, M = monomer, I = initiator, B = buffer

Table 3 Volume (d_v) and area (d_a) average diameters, polydispersity indexes (PDI) and surface charge densities (σ_o) obtained for each run

Run	d_v (nm)	d_a (nm)	PDI	σ_0 ($\mu C\,cm^{-2}$)
E1	103	97	1.42	1.50
E2	129	120	1.59	0.73
E3	124	119	1.29	2.15
E4	104	100	1.29	3.90
E9	115	110	1.23	0.55
EU	252	251	1.04	7.20
EV	103	97	1.44	2.53
EAE	143	139	1.20	1.52

Table 4 CCC values at three different pH and surface charge densities [weak acid (w), strong acid (s) and total (0) of the latex particles

Latex	σ_w (μC cm^{-2})	σ_s (μC cm^{-2})	σ_0 (μC cm^{-2})	pH	CCC(M)	
E1	–	1.50	1.50	5	0.19	
				7	0.20	
				9	0.25	
E3	1.60	0.55	2.15	5	0.14	
				7	0.22	
				9	0.22	Seeded
E4	1.95	1.95	3.90	5	0.21	
				7	0.34	
				9	0.50	
E9	–	0.55	0.55	5	0.06	
				7	0.06	
				9	0.06	
E2	–	0.73	0.73	5	0.04	
				7	0.06	
				9	0.06	
EV	1.13	1.40	2.53	5	0.15	
				7	0.20	Unseeded
				9	0.23	
EAE	–	1.52	1.52	5	0.10	
				7	0.10	
				9	0.18	

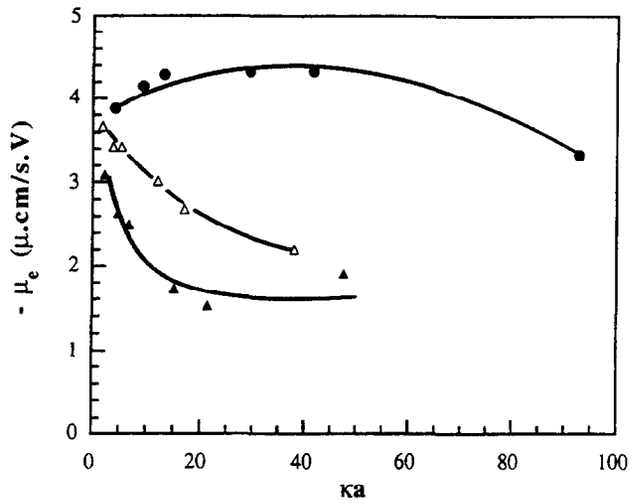

Figure 1 Electrophoretic mobility values vs. electrokinetic radius. (▲) Latex E2, (△) latex EV, (●) latex EU

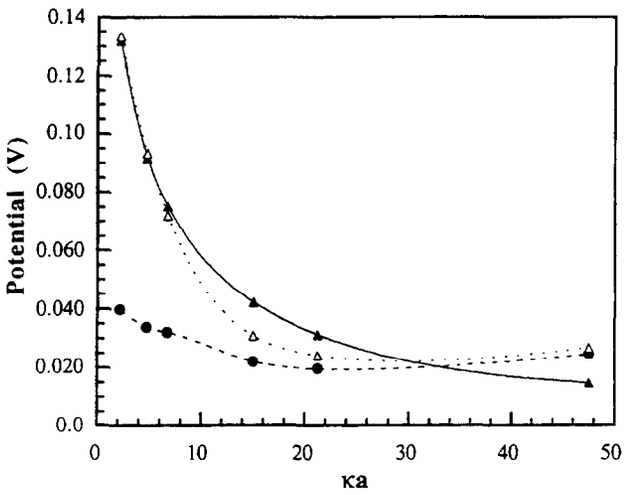

Figure 2 Electric potential vs. electrokinetic radius for the latex E2. (▲) Diffuse potential, (●) ζ-potential (Smoluchowski), (△) ζ-potential (Dukhin–Semenikhin)

RESULTS AND DISCUSSION

Electrophoretic mobility

Figure 1 shows the electrophoretic mobility values for three of the latexes (with highest, EU, intermediate, EV, and lowest, E2, surface charge) as a function of the electrokinetic radius. The other latexes showed an intermediate behaviour. The different κa values were obtained by varying the concentration of the 1/1 electrolyte. The μ_e–κa curve passes through a wide maximum at κa values between 30 and 50 for latex EU (highest surface charge), whereas latex E2 (lowest surface charge) displays an electrokinetic behaviour in good agreement with the Gouy–Chapman theory.

The conversion of mobility into ζ-potential of latex–aqueous interface encounter at least three obstacles which must be dealt with: polarization of the electric double layer (e.d.l.) in an external field, the possible existence of a boundary layer with reduced hydrodynamic mobility, and the significant roughness of the latex surface. These difficulties can be partly overcome by using the theories developed for non-equilibrium electrosurface phenomena. But the description of the spatial structure of the deformed e.d.l., essential for the derivation of the electrophoresis relationships, is complicated by the fact that the Boltzmann distribution cannot be used *a priori*. Moreover, even when the stationary state is attained, ionic flows in the e.d.l. do not vanish, so that valid application of the Boltzmann distribution cannot *a priori* be assumed[7]. Overbeek[9]

and Booth[10] were the first to incorporate e.d.l. polarization into the theory. O'Brien and White[11], starting from the same set of equations as Wiersema[12], have more recently published a theoretical approach to electrophoresis, taking into account any combination of ions in solution and the possibility of very high ζ-potentials (up to 250 mV), far enough from the values to be expected in most experimental conditions. They assumed that the transfer and charge distribution processes only take place in the mobile part of the e.d.l. All the above cited theoretical approaches convert mobility into ζ-potential on the basis that there is no ionic conduction inside the shear plane. In an attempt to account theoretically for this phenomenon, Dukhin–Semenikhin[13] developed an equation incorporating both the dimensionless $\tilde{\zeta}$-potential and the dimensionless diffuse potential ($\tilde{\Psi}_d$-potential). The value of dimensionless electrophoretic mobility for a spherical particle with a thin e.d.l. in a 1/1 electrolyte is given by

$$\tilde{\mu}_e = \frac{3}{2}\tilde{\zeta}\left[\frac{1 + Rel(4\ln\cos[(\tilde{\zeta}/4))/\tilde{\zeta}]}{1 + 2Rel}\right] \quad (1)$$

where

$$Rel = \frac{\lambda_s}{\lambda a} = \frac{\exp(\tilde{\Psi}_d/2) + 3m\exp(\tilde{\zeta}/2)}{\kappa a} \quad (2)$$

The dimensionless relaxation parameter *Rel* can be interpreted in two ways: as a measure for the degree of e.d.l. polarization (non-equilibrium degree) for curved surfaces or for the relative contribution of surface conductance in non-polarized systems (equilibrium states). The main advantage of the Dukhin–Semenikhin theory is that it allows us to take the effect of anomalous conduction on e.d.l. polarization into account.

The calculation of ζ with allowance for e.d.l. polarization within the framework of the Dukhin–Semenikhin theory requires a knowledge of the Ψ_d-potential, which can be used on the basis of σ_o[7].

$$\sigma_0 = \left(\frac{2\epsilon nkT}{\pi}\right)^{1/2}\left[\sinh\frac{\tilde{\Psi}_d}{2} + \frac{2}{\kappa a}\tanh\frac{\tilde{\Psi}_d}{4}\right] \quad (3)$$

From the plots shown in *Figures 2*, *3* and *4*, for ζ_{Sm}, ζ_{D-S}, Ψ_d as functions of the electrokinetic radius, we see that the ζ-potential calculated with allowance for e.d.l. polarization is substantially greater than ζ calculated according to the classical Smoluchowski equation. These differences gradually smooth out as the e.d.l. becomes thinner, as could be expected.

Figure 5 shows the dependence of the electrophoretic mobility on surface charge density for three different ionic strengths. In all cases the behaviour is quite similar; a sharp increase of mobility with surface charge density at densities below $2\,\mu C\,cm^{-2}$, constant mobility in the range from 2 to $6\,\mu C\,cm^{-2}$ and slight increase at higher charge values. The mobility increases at low ionic strength, when, obviously, electrostatic interactions in the e.d.l. are more effective. This plateau value of mobility agrees with the prediction of Lyklema[14]. This plateau is almost independent of the nature of the surface and can be explained in terms of the viscoelectric effect, i.e. the increase in viscosity η of a polar liquid caused by an applied field. According to this idea the e.d.l. field is

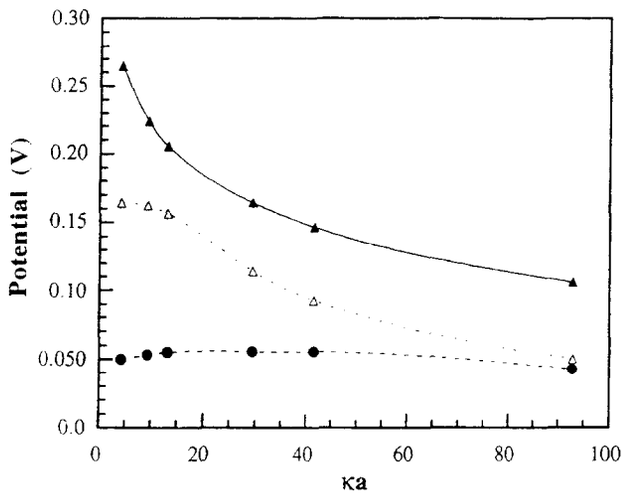

Figure 4 Electric potential vs. electrokinetic radius for the latex EU. (▲) Diffuse potential, (●) ζ-potential (Smoluchowski), (△) ζ-potential (Dukhin–Semenikhin)

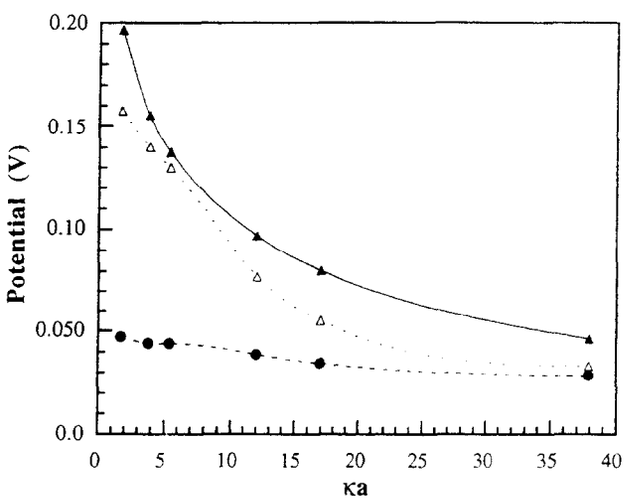

Figure 3 Electric potential values vs. electrokinetic radius for the latex EV. (▲) Diffuse potential, (●) ζ-potential (Smoluchowski), (△) ζ-potential (Dukhin–Semenikhin)

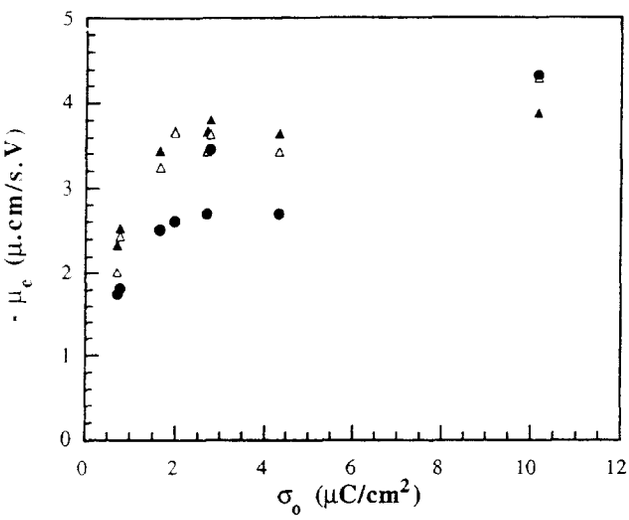

Figure 5 Electrophoretic mobility values vs. surface charge density at different ionic strengths. (●) $C_{KBr} = 10^{-2}$ M, (△) $C_{KBr} = 10^{-3}$ M, (▲) $C_{KBr} = 10^{-4}$ M

responsible for an increase of the liquid viscosity (η) close to the surface, so as to suppress tangential flow in that region. The viscoelectric effect already sets in at field strengths of the order of $10^5\,V\,cm^{-1}$, one order of magnitude less than for the dielectric permittivity. Because of the viscoelectric effect, there is a critical field strength in the double layer above which the liquid is virtually immobilized. This explains why the mobility is constant above $2.5\,\mu C\,cm^{-2}$ of electrokinetic charge, as predicted by Lyklema[14].

In *Figure 6*, the *Rel* factor has been plotted as a function of the electrokinetic radius. As can be seen, this term is larger at low κa. This means that the double layer relaxation and, hence the anomalous surface conductance, are proportional to the e.d.l. thickness, and for the latexes its contribution drops off substantially as the e.d.l. is compressed, and becomes negligibly small with $\kappa a \geq 50$; as a consequence, the difference between the ζ_{Sm} and ζ_{D-S} zeta potentials disappears.

An important result of the combined measurements made is that even when the ζ-potentials are corrected for the e.d.l. polarization, the values for the latex–solution interfaces are less than Ψ_d over a wide range of electrokinetic radius, which occurs mainly with highly charged latexes (see *Figure 4*). This may be due to the formation of a liquid layer on the latex particle surface with low hydrodynamic mobility, in which the ions retain high mobility. The thickness of this layer, Δ, can be estimated by the relationship obtained by Eversole and Boardman[15]

$$\tanh(\tilde{\zeta}/4) = \tanh(\tilde{\Psi}_d/4)\exp(-\kappa\Delta) \qquad (4)$$

This equation assumes that the ions near a charged wall are subjected only to electrostatic and kinetic forces, and is based on the fact that the potential gradient normal to the wall is determined principally by the valence and the concentration of the ion of opposite charge to that of the wall. Assuming that the valence and the concentration of this ion determine the effect of the salt on the electrokinetic and diffuse potentials of the wall, the thickness of the immobilized liquid layer can be calculated from these potential data.

A calculation based on this relationship with the values found for Ψ_d and ζ_{D-S} shows that the thickness of this water layer is 2.0 nm for the most charged latex–water interface, and 1.2 for the least charged one. Obviously, the most charged latex shows a thicker water layer around the beads. The importance of the vicinal water around polymer beads has been pointed out by other authors[16–18].

The differences between the Ψ_d and ζ potentials seem to indicate that, between the outer Helmholtz and the shear planes, there is charge which could be responsible for λ_s.

Colloidal stability

In *Table 4*, the values of the CCC of the synthesized latexes at pH 5, 7 and 9, and the surface charge densities are shown. Two latexes, E2 and E9, have a CCC equal to 0.06 M and independent of pH. As can be seen, the higher the surface charge density, the greater the CCC values. The highest charged latex E4 (with a charge of $3.90\,\mu C\,cm^{-2}$), has an increased CCC, especially at pH = 9.

In *Figure 7*, the values of the CCCs with pH are shown. In the case of the latexes with low surface charge densities (less than $1\,\mu C\,cm^{-2}$), E2 and E9, their CCCs are low and do not change at different pH values. The most highly charged latex, E4, has a CCC that changes with pH. The greater the pH, the higher the CCC. The other latexes also show this increase in the CCC with the pH, but to a lesser extent.

A higher stability is expected at basic pH, at which the surface charge is higher. When the pH is lower, the surface acid groups, above all, the weak acid ones, are partially protonated diminishing the surface charge and the stability. Under these conditions, the differences between the latexes are smaller.

The E2 and E9 latexes have only strong acid surface groups provided by the initiator, and over the pH range studied, they are not protonated. Due to this, both the surface charge density and the CCC are pH independent.

The latexes with weak acid surface groups, specifically the E4, have their surface charge and CCC very pH sensitive.

These results indicated that the stabilizing mechanism of the latexes studied is only electrostatic. The largest

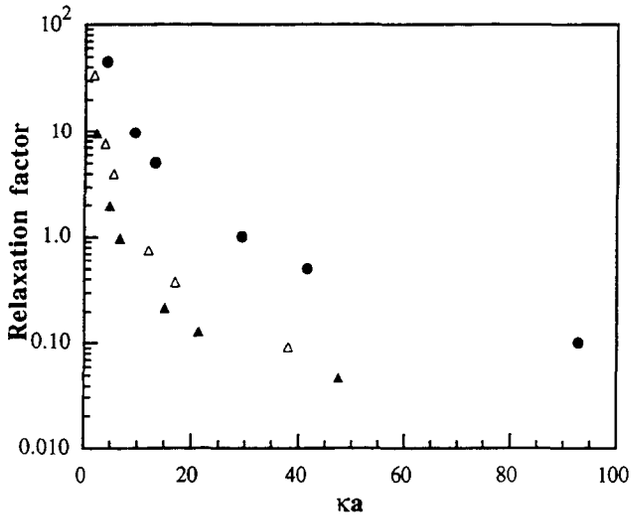

Figure 6 Relaxation factor (*Rel*) values vs. electrokinetic radius. (▲) Latex E2, (△) latex EV, (●) latex EU

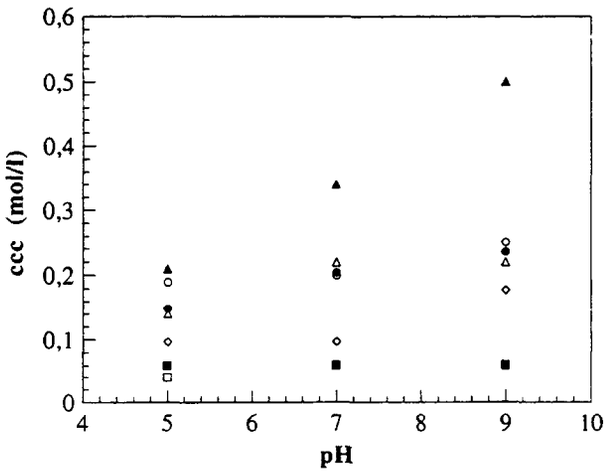

Figure 7 Values of the CCCs at different pH. (○) Latex E1, (□) latex E2, (△) latex E3, (▲) latex E4, (■) latex E9, (●) latex EV, (◇) latex EAE

CCC values are obtained with the SLS–Gafac mixture, and the colloidal stability depends on the surfactant mixture. The polymerizing method (seeded or unseeded) does not affect the stabilizing mechanism of the latexes studied.

CONCLUSIONS

Polymethyl methacrylate-*co*-butyl acrylate latexes were prepared by semicontinuous emulsion copolymerization at 60°C.

The characterization of the cleaned latexes included surface charge densities, average particle diameters and electrophoretic mobilities. The conversion of electrophoretic mobility into ζ-potentials for electrokinetic radii between 5 and 50 should be made by a non-equilibrium theory that includes the inherent anomalous surface conductance of the polymer beads–electrolyte solution interface. This is partly satisfied by the Dukhin–Semenikhin theory, since it takes into account the anomalous surface conductance associated with the presence of a boundary layer.

The colloidal stability of the latex particles obtained is only due to electrostatic forces. The polymerization method (seeded or unseeded) of the latex particles does not affect their stability in a colloidal sense.

LIST OF PRINCIPAL SYMBOLS

a	particle radius
D	diffusion coefficient
e	elemental electric charge
k	Boltzmann constant
m	dimensionless ionic drag coefficient $((2\epsilon/3\eta D)(kT/e)^2)$
n	ionic concentration
Rel	double layer relaxation factor
T	absolute temperature
ϵ	dielectric permittivity of the continuous phase
η	liquid viscosity
κ	reciprocal of the electrical double layer thickness (Debye-Hückel length)
λ	specific electrical conductivity
λ_s	surface electrical conductance
σ_o	surface charge density
μ_e	microelectrophoretic mobility
$\tilde{\mu}_e$	dimensionless microelectrophoretic mobility
Ψ_d	diffuse layer potential
$\tilde{\Psi}_d$	dimensionless diffuse layer potential
$\tilde{\zeta} = e/kT$	dimensionless electrokinetic potential
Δ	thickness of hydrodynamically rigid layer at the solid phase

ACKNOWLEDGEMENTS

The authors gratefully acknowledge the financial support of the Comisión Interministerial de Ciencia y Tecnología (CICYT), project MAT 96-1035-CO3-01 and 02.

E. Unzueta and J. Forcada would like to thank Eusko Jaurlaritza (PI 94/6) and Universidad del País Vasco/Euskal Herriko Unibertsitatea (PI 221215 EA 062/92), for their financial support.

R. Hidalgo-Álvarez wishes to express his gratitude for the financial support of the Junta de Andalucía (PA, Grupo 1218).

REFERENCES

1. *Preparation, Properties and Uses of Acrylic Polymers*, CM-19. Rohm and Haas Co., Philadelphia.
2. Mercurio, A. and Lewis, S. N., *J. Paint Technol.*, 1975, **47**, 37.
3. Unzueta, E. and Forcada, J., *Polymer*, 1995, **36**(5), 1045.
4. Unzueta, E. and Forcada, J., *Polymer*, 1995, **36**(22), 4301.
5. Hidalgo-Álvarez, R., de las Nieves, F. J., Van der Linde, A. J. and Bijsterbosch, B. H., *Colloids Surfaces*, 1986, **21**, 259.
6. Goff, J. R. and Luner, Ph. J., *J. Colloid Interface Sci.*, 1984, **99**, 468.
7. Dukhin, S. S. and Derjaguin, B. V., *Surface and Colloid Science*, Vol 7, ed. E. Matijevic. Wiley, New York, 1974.
8. Bastos, D. and de las Nieves, F. J., *Colloid Polym. Sci.*, 1994, **272**, 592.
9. Overbeek, J. Th. G., *Adv. Colloid Sci.*, 1950, **1**, 514.
10. Booth, F., *Proc. Soc. London Ser. A*, 1950, **203**, 514.
11. O'Brien, R. W. and White, L. R., *J. Chem. Soc. Faraday II* 1978, **77**, 1607.
12. Wiersema, P. H., Loeb, A. L., Overbeek, J. Th. G., *J. Colloid Interface Sci.*, 1966, **22**, 78.
13. Semenikhin, N. M. and Dukhin, S. S., *Kolloidn Zh.*, 1975, **37**, 1017.
14. Lyklema, J., *Colloids Surfaces A: Physicochem. Engn. Aspects*, 1994, **92**, 41.
15. Eversole, W. G. and Boardman, W. W., *J. Chem. Phys.*, 1941, **9**, 798.
16. Hidalgo-Álvarez, R., *Adv. Colloid Interface Sci.*, 1991, **34**, 217.
17. Baran, A. A., Dudkina, L. M., Soboleva, N. M. and Chechnik, O. S., *Kolloidn Zh.*, 1981, **43**, 211.
18. Midmore, B. R. and Hunter, R. J., *J. Colloid Interface Sci.*, 1988, **122**, 211.